



# Nuclear Spin Isomers: Engineering a $\text{Et}_4\text{N}[\text{DyPc}_2]$ Spin Qudit

Eufemio Moreno-Pineda,\* Marko Damjanović, Olaf Fuhr, Wolfgang Wernsdorfer,\* and Mario Ruben\*

**Abstract:** Two dysprosium isotopic isomers were synthesized:  $\text{Et}_4\text{N}[\text{Dy}^{163}\text{Pc}_2]$  (**1**) with  $I=5/2$  and  $\text{Et}_4\text{N}[\text{Dy}^{164}\text{Pc}_2]$  (**2**) with  $I=0$  (where Pc = phthalocyaninato). Both isotopologues are single-molecule magnets (SMMs); however, their relaxation times as well as their magnetic hystereses differ considerably. Quantum tunneling of the magnetization (QTM) at the energy level crossings is found for both systems via ac-susceptibility and  $\mu$ -SQUID measurements.  $\mu$ -SQUID studies of **1** ( $I=5/2$ ) reveal several nuclear-spin-driven QTM events; hence determination of the hyperfine coupling and the nuclear quadrupole splitting is possible. Compound **2** ( $I=0$ ) shows only strongly reduced QTM at zero magnetic field. **1** ( $I=5/2$ ) could be used as a multilevel nuclear spin qubit, namely qudit ( $d=6$ ), for quantum information processing (QIP) schemes and provides an example of novel coordination-chemistry-discriminating nuclear spin isotopes. Our results show that the nuclear spin of the lanthanide must be included in the design principles of molecular qubits and SMMs.

Since the discovery of magnetic memory at the single-ion level,<sup>[1]</sup> several applications have been foreseen for lanthanide-based single-molecule magnets (Ln-SMMs), ranging from data storage<sup>[2]</sup> to spintronic devices.<sup>[3a]</sup> Amongst the many conceivable applications, probably the most ambitious one is related to the integration of Ln-SMMs in quantum information schemes acting as quantum bits (qubits).<sup>[3–5]</sup> Although seemingly a long-term goal, in fact Ln-SMMs have already shown several of the required DiVincenzo characteristics<sup>[6]</sup> needed to perform as nuclear spin qubits.<sup>[3,5]</sup>

The richness of quantum effects observed in Ln-SMMs and their possible applications in quantum technologies is best exemplified by the family of terbium bis(phthalocyaninato) complexes.<sup>[3]</sup> In the  $[\text{TbPc}_2]^{0,\pm 1}$ , the strong magnetic anisotropy arises from a combination of the spin-orbit coupling of the  $\text{Tb}^{\text{III}}$  ion and the ligand field (LF) induced by the phthalocyaninato moieties. The SMM property isolates the ground electronic state from excited states, while the strong hyperfine interaction allows the direct observation of the nuclear spin states of the  $\text{Tb}^{\text{III}}$  ion. At the level crossings, the nuclear spin states are observed as QTM events, which are induced by the transverse LF terms. The QTM occurs due to reversal of the electronic spin, while the nuclear spin state is unchanged.<sup>[7]</sup> Integration of  $[\text{TbPc}_2]^{0,\pm 1}$  in hybrid devices has allowed the initialization, manipulation, and read-out of the nuclear spin states, making it a promising multilevel nuclear spin qubit,<sup>[3a]</sup> or qudit ( $d=4$ ) for  $d$ -dimensional systems.<sup>[4]</sup> This is due to the inherent shielding of nuclear spins from the environment, which yields unusually long coherence times and low error rates.<sup>[3,9]</sup> Moreover, the multilevel nuclear-spin characteristic of  $[\text{TbPc}_2]^{0,\pm 1}$  has been proposed for quantum-based data search schemes in unsorted databases, the so-called “Grover Algorithm”.<sup>[5,10]</sup> This algorithm makes it possible to exploit the superposition of the nuclear spin states through a Hadamard gate, accelerating search times.<sup>[11]</sup>

As described above, the strong magnetic anisotropy is a precondition for the successful initialization, manipulation and read-out of the nuclear states in the Tb-SMM, allowing them to act as qubits. In this sense, Tb-based SMMs seem to be promising candidates as nuclear spin qubits. However, due to the non-Kramers character of the  $\text{Tb}^{\text{III}}$  ion, only very scarce examples of Tb-SMMs exist.<sup>[12]</sup> Conversely, the neighboring  $\text{Dy}^{\text{III}}$  ion has become the leading lanthanide for the synthesis of SMMs.<sup>[13]</sup> The favorable Kramers characteristic of  $\text{Dy}^{\text{III}}$  often yields well-isolated ground doublet state.<sup>[12,13]</sup> Unfortunately, the advantageous magnetic properties of  $\text{Dy}^{\text{III}}$  ions come at a price: whereas  $^{159}\text{Tb}^{\text{III}}$  contains a single nuclear spin isotope,  $I=3/2$ , with 100% natural abundance, the natural composition of  $\text{Dy}^{\text{III}}$  comprises seven isotopes, possessing two different nuclear spin states,  $I=0$  and  $5/2$ . Recently, in the quest for materials with improved SMM properties, some research groups exploited the synthesis of isotopically enriched Dy-SMMs to enhance the magnetic hysteresis width by excluding nuclear spins.<sup>[14]</sup> The utilization of  $^{164}\text{Dy}^{\text{III}}$  ( $I=0$ ) led to the observation of enlarged hysteresis loops at zero field, in comparison to SMMs obtained from the naturally occurring isotopic mixture. On the contrary, investigation of the nuclear-spin-bearing materials, their quantum properties, and their basic studies for their application as nuclear spin qubits remain scarce.<sup>[3a,6,14,15]</sup>

Herein, we describe the low-temperature magnetic properties of two isotopically enriched versions of the prototype anionic  $[\text{DyPc}_2]^-$  SMM:  $\text{Et}_4\text{N}[\text{Dy}^{163}\text{Pc}_2]$  (**1**) ( $I=5/2$ ) and  $\text{Et}_4\text{N}[\text{Dy}^{164}\text{Pc}_2]$  (**2**) ( $I=0$ ) with  $I=5/2$  and  $I=0$ , respectively

[\*] Dr. E. Moreno-Pineda, Dr. M. Damjanović, Dr. O. Fuhr, Prof. Dr. W. Wernsdorfer, Prof. Dr. M. Ruben  
Institute of Nanotechnology (INT)  
Karlsruhe Institute of Technology (KIT)  
Hermann-von-Helmholtz-Platz 1, 76344 Eggenstein-Leopoldshafen  
(Germany)  
E-mail: eufemio.pineda@kit.edu  
wolfgang.wernsdorfer@kit.edu  
mario.ruben@kit.edu

Prof. Dr. W. Wernsdorfer  
Institut Néel, CNRS, Université Grenoble Alpes  
25 rue des Martyrs, 38000 Grenoble (France)  
Prof. Dr. M. Ruben  
Institut de Physique et Chimie des Matériaux de Strasbourg (IPCMS)  
CNRS, Université de Strasbourg  
23 rue du Loess, BP 43, 67034 Strasbourg Cedex 2 (France)

Supporting information and the ORCID identification number(s) for the author(s) of this article can be found under:  
<https://doi.org/10.1002/anie.201706181>.

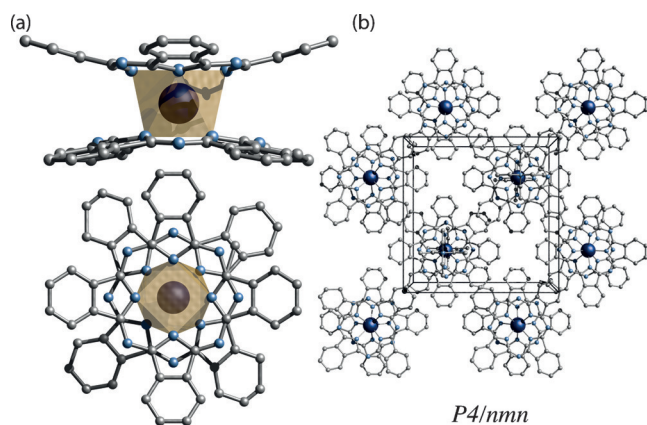


**Figure 1.** a) Side (top) and top (bottom) view of the crystal structures of the isotopologues  $\text{Et}_4\text{N}[\text{Dy}^{163}\text{Pc}_2]$  (**1**) and  $\text{Et}_4\text{N}[\text{Dy}^{164}\text{Pc}_2]$  (**2**). Both  $\text{Dy}^{\text{III}}$  ion isotopes possess  $D_{4d}$  symmetry. Gold-colored regions represent the square antiprismatic coordination geometry of the Dy ions. b) Packing of **1** and **2** molecules in the tetragonal unit cell. Color code: Dy dark blue, N cyan, C gray. H atoms omitted for clarity.

(Figure 1). Nuclear-spin-driven QTM events are found for the  $\text{Et}_4\text{N}[\text{Dy}^{163}\text{Pc}_2]$  compound via alternating current (AC) studies and low-temperature  $\mu$ -SQUID measurements.

Compounds **1** and **2** comprise isostructural double-deckers motifs and crystallize in the tetragonal  $P4/nmm$  space group with one half of the molecule per asymmetric unit. The Dy $\cdots$ N distances are similar in both cases with 2.414(5)–2.415(4) Å and 2.418(5)–2.422(5) Å for **1** and **2**, respectively. Locally, each  $\text{Dy}^{\text{III}}$  ion possesses a  $D_{4d}$  coordination geometry with CShM values<sup>[16]</sup> of 0.580 and 0.560 for **1** and **2**, respectively. The anionic complexes are charge-balanced by a tetraethylammonium cation.

In our study, we first explored the dynamic magnetic properties of **1** and **2** through AC magnetic susceptibility measurements (details are provided in the Supporting Information). The studies were performed on 5% diluted samples to reduce intermolecular effects, known to play a relevant role in the relaxation of SMMs.<sup>[17]</sup> To this end, magnetic dilution was achieved with the yttrium diamagnetic analogue  $\text{Et}_4\text{N}[\text{YPC}_2]$  (**3**), leading to:  $\text{Et}_4\text{N}[\text{Dy}_{0.05}\text{Y}_{0.95}\text{Pc}_2]$  (**1a**) and  $\text{Et}_4\text{N}[\text{Dy}_{0.05}\text{Y}_{0.95}\text{Pc}_2]$  (**2a**) (see the Supporting Information for details). At zero field, both complexes exhibit the expected frequency-dependent behavior characteristic of SMMs.<sup>[18]</sup> Small differences are barely observed in the out-of-phase component ( $\chi''(\nu)$ ): compound **1a** tunnels faster than compound **2a**, as observed in the maximum starting at 0.22 Hz (at 2 K) for **1a**, compared to 0.1 Hz (at 2 K) for complex **2a**. This small difference is expected due to the local magnetic field generated by the  $\text{Dy}^{\text{III}}$  nuclear spin in **1a**, which enhances QTM (Figure 2a,b). Analogously, the  $\chi''(\nu)$  of **1a** reaches 8 K, whereas for **2a** it extends up to 9.2 K. Fitting the  $\chi''(\nu)$  data to a single process followed by an Arrhenius analysis affords  $U_{\text{eff}} = 34.5(3)$  K,  $\tau_0 = 1.60(1) \times 10^{-6}$  s for **1a** and  $U_{\text{eff}} = 34.7(5)$  K,  $\tau_0 = 2.9(1) \times 10^{-6}$  s for **2a** (Figure 2c). The  $\alpha$  parameters obtained from Cole–Cole plots reveal a narrow

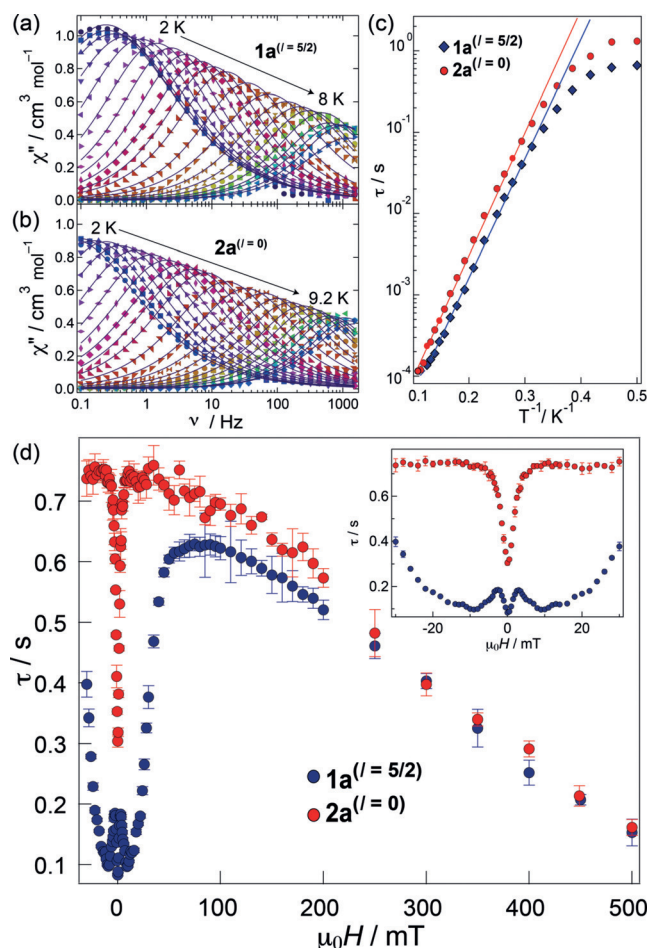


**Figure 2.** a,b)  $\chi''(\nu)$  experimental data for **1a** and **2a**, respectively, with  $H_{\text{DC}} = 0$  and an oscillating field of 3.5 Oe. Solid lines are fits to a single Debye process. c)  $\tau(T)$  data for **1a** (blue) and **2a** (red) and Arrhenius analysis (solid lines). d)  $\tau(H)$  data for **1a** (blue) and **2a** (red). Inset shows  $\tau(H)$  data at low field.

distribution of relaxation times ( $\tau$ ):  $0.46 > \alpha_{1a} > 0.16$  and  $0.48 > \alpha_{2a} > 0.13$ .

To examine  $\tau$  in detail, field-dependent studies, that is,  $\tau(H)$ , were conducted at 3 K with fields ranging from  $-30$  mT to  $+500$  mT. Under these conditions, the  $\tau(H)$  for **1a** and **2a** exhibits a field-dependent tendency: with increasing fields  $\tau$  increases due to suppression of QTM, whilst at higher fields  $\tau$  decreases due to direct relaxation processes. Note that the  $\tau(H)$  of **1a** in the range of  $\pm 30$  mT displays a fine structure, suggesting that hyperfine interactions could play a major role in the QTM (inset in Figure 2d), whereas for **2a** a smooth decrease in  $\tau$  is observed with the minimum value at zero field. The behavior for **1a** is expected due to the presence of the  $\text{Dy}^{\text{III}}$  nuclear spin, which allows spin flips via the avoided level crossings,<sup>[8]</sup> whilst the drop of  $\tau(H)$  in **2a** could be caused by transverse anisotropy, hyperfine interactions with neighboring atoms, for example,  $^{14}\text{N}$  ( $I = 1$ ) of the  $\text{Pc}^{2-}$  ligands, and/or dipolar fields not fully suppressed at 5% magnetic dilution.

To further explore the magnetic behavior of **1a** and **2a**, and more importantly the low-field structure observed in the  $\tau(H)$  of **1a**,  $\mu$ -SQUID measurements on single

crystals were carried out.<sup>[19a]</sup> In both cases, the field was aligned parallel to the easy axis of magnetization.<sup>[19b]</sup> Hysteresis loops studies were performed at different sweep rates and temperatures (Figure 3 and Figure S6). First, we compare

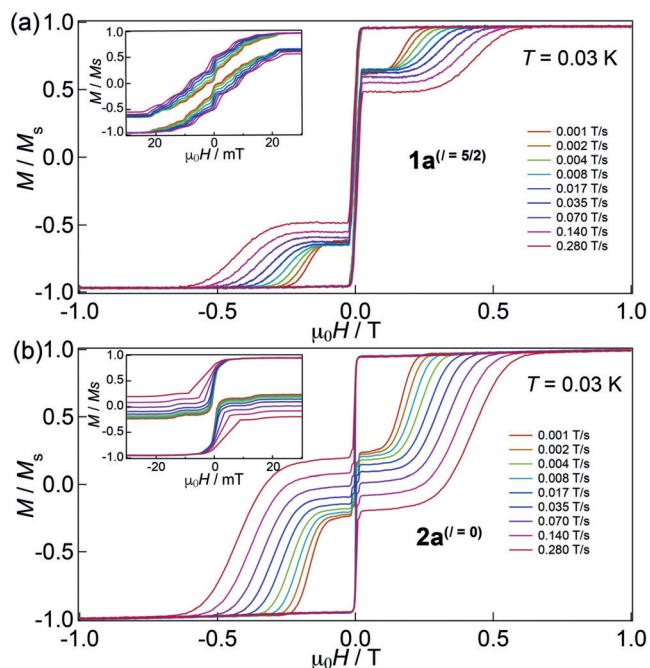


**Figure 3.** Field dependence of the magnetization at  $T = 0.03$  K with the field applied parallel to the easy axis of the magnetization: a)  $\mathbf{1a}^{(I=5/2)}$  and b)  $\mathbf{2a}^{(I=0)}$ . Insets show magnified regions between  $\pm 30$  mT.

the width of the hysteresis loops, where slightly wider hystereses are observed for  $\mathbf{2a}^{(I=0)}$  (cf.  $\mathbf{1a}^{(I=5/2)}$ ) at  $\mu_0 H \neq 0$ , due to the lack of the  $\text{Dy}^{\text{III}}$  nuclear spin. Note that despite the absence of the nuclear spin in  $\mathbf{2a}^{(I=0)}$  and the Kramers spin parity character,  $\mathbf{2a}^{(I=0)}$  tunnels sharply at zero field. This shows that hyperfine interactions with adjacent atoms and/or dipolar interactions can still induce QTM.<sup>[14,17]</sup>

In contrast, as shown in the inset of Figure 3a, the  $\mu$ -SQUID loops for  $\mathbf{1a}^{(I=5/2)}$  reveal a staircase-like structure between ca.  $\pm 20$  mT (cf. insets in Figure 3a,b), which is clear evidence of hyperfine-induced QTM events. In this case, QTM arises from the non-zero transverse terms under  $C_4$  symmetry, that is, the terms  $A_4^4 \langle r^4 \rangle O_4^4$  and  $A_6^4 \langle r^4 \rangle O_6^4$ , (where  $\hat{O}_k^n$  are the Stevens operators and  $A_k^n$  are ligand field parameters).<sup>[20]</sup> These terms allow the admixtures of the off-diagonal elements, which mix the  $|J_z\rangle$  and the  $|J_z - 4\rangle$  levels affording an avoided crossing at zero field.<sup>[20]</sup> This crossing is further split, due to the entanglement between the  $|13/2\rangle$  electronic and the  $I = 5/2$  nuclear spin in  $\mathbf{1a}^{(I=5/2)}$ . A total of 36 level crossings are expected (Figure 4c). Most of the tunneling events can be explained by a hyperfine interaction ( $A_{\text{hf}}$ ) and a quadrupole term ( $P$ ), employing a Hamiltonian of the form given in Equation (1)

$$\mathcal{H} = \mathcal{H}_{\text{hf}} + g_I \mu_0 \mu_B \mathbf{J} \cdot \mathbf{H} + A_{\text{hf}} \mathbf{I} \cdot \mathbf{J} + P \left( I_z^2 - \frac{1}{3} (I+1) \mathbf{I} \right) \quad (1)$$

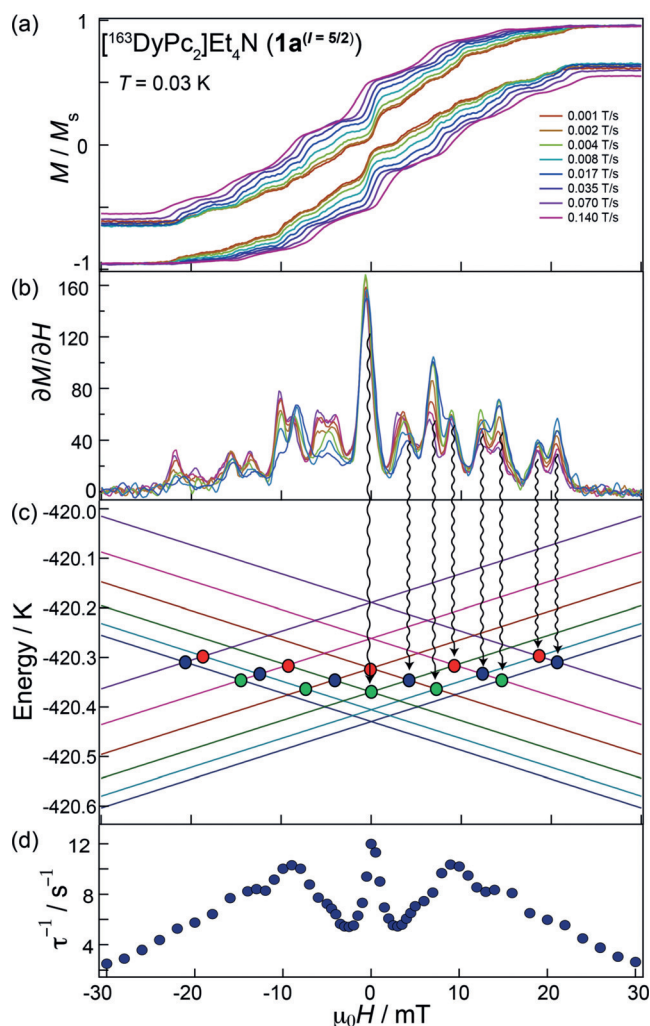


**Figure 4.** a) Hysteresis loops at  $T = 0.03$  K for  $\mathbf{1a}^{(I=5/2)}$  between  $\pm 30$  mT showing the staircase-like structure. b) First derivative of the magnetization of  $\mu$ -SQUID loops shown in panel (a). c) Simulated Zeeman diagram with the field parallel to the easy axes of  $\mathbf{1a}^{(I=5/2)}$ , employing Equation (1) and parameters reported in Ref.[17b]. Electronic spin flips are observed when:  $\Delta m_I = -1$  (green circles);  $\Delta m_I = 0$  (blue circles) and  $\Delta m_I = +1$  (red circles). d) Field dependence of the inverse relaxation time,  $\tau^{-1}(H)$ , for compound  $\mathbf{1a}^{(I=5/2)}$  in the field range of  $\pm 30$  mT.

where  $\mathcal{H}_{\text{hf}}$  is the LF Hamiltonian ( $\mathcal{H}_{\text{hf}} = \alpha A_2^0 O_2^0 + \beta (A_4^0 O_4^0 + A_4^4 O_4^4) + \gamma (A_6^0 O_6^0 + A_6^4 O_6^4)$  in which  $\alpha$ ,  $\beta$ , and  $\gamma$  are the Stevens constants). The second term describes the Zeeman interaction, followed by the hyperfine and the quadrupole interaction parameters. Employing the reported LF values,<sup>[8,18b]</sup> a hyperfine parameter,  $A_{\text{hf}} = 0.0051 \text{ cm}^{-1}$  and a quadrupole value of  $P = 0.014 \text{ cm}^{-1}$  we are able to reproduce the observed events.

For a  $C_4$  symmetry, QTM is allowed just at five crossings (green circles in Figure 4c). These are caused by the presence of transverse terms in Equation (1). At these five intersections, the electronic spin is reversed whilst the nuclear spin increases by one unit, that is,  $| -13/2 \rangle | I_z \rangle \leftrightarrow | +13/2 \rangle | I_z + 1 \rangle$ . Interestingly, 10 additional events are present, which could be associated to spin-spin cross relaxation (SSCR), known to be

enhanced via dipolar and super-exchange interactions.<sup>[21]</sup> The additional QTM occurrences can be ascribed to electronic spin flips with no variation of the nuclear spin (blue circles in Figure 4c), that is,  $| -13/2 \rangle | I_z \rangle \leftrightarrow | +13/2 \rangle | I_z \rangle$  and electronic spin flips while the nuclear spin decreases by one unit,  $| -13/2 \rangle | I_z \rangle \leftrightarrow | +13/2 \rangle | I_z - 1 \rangle$ , (red circles in Figure 4b).

At this point, we are able to correlate the fine structure for  $1\mathbf{a}^{(I=5/2)}$  obtained from AC measurements that is,  $\tau(H)$ , with the  $\mu$ -SQUID data. Both sets of data show similar profiles (cf. Figure 4b and d). As observed in Figure 4c, at zero field QTM is readily available. Upon application of a small magnetic field, QTM decreases, therefore  $\tau$  increases. This effect is observed until the applied field matches the field at the first avoided crossing, therefore increasing QTM, that is,  $\tau$  decreases. Due to the several level crossings, a fluctuating behavior is observed in the whole  $\tau(H)$  range. Nevertheless, given that the  $\tau(H)$  study was carried out on a powdered sample, the crossings at specific resonance fields are expectedly smeared out (cf. Figure 4b).

In summary, two SMMs have been engineered, which could be employed in spintronic and in QIP schemes. Detailed studies of  $2\mathbf{a}^{(I=0)}$  shows slightly enlarged hystereses for non-zero applied fields due to the suppression of nuclear-spin-enhanced QTM. Note that, although the study was conducted on magnetically diluted samples, QTM is still active at zero field. This confirms that hyperfine and/or dipolar interactions still play an active role in the relaxation of the magnetization. Moreover, detailed studies of the  $\tau(H)$  from AC data from  $1\mathbf{a}^{(I=5/2)}$  reveals nuclear-spin-associated QTM events. These findings are in very good agreement with the  $\mu$ -SQUID results. More importantly, due to the observation of QTM associated to the nuclear spin of  $\text{Dy}^{\text{III}}$ , this molecular magnet represents a promising molecular nuclear spin qudit ( $d=6$  for a Hilbert space of dimension  $2^{d+1}$ ) where the absolute value of the quadrupolar term is 40% larger than the observed in prototypical  $[\text{TbPc}_2]^{0,\pm 1}$  qudit.<sup>[8]</sup> In addition to the strength of the quadrupole term, the multiplicity of nuclear spin states ( $m_I = \pm 5/2, \pm 3/2, \text{ and } \pm 1/2$ ) makes  $\text{Et}_4\text{N}^{163}\text{DyPc}_2$  a very promising candidate for the implementation of the Grover algorithm, even better than  $[\text{TbPc}_2]^{0,\pm 1}$  with only  $m_I = \pm 3/2, \pm 1/2$  states.<sup>[3c,5,10]</sup> In conclusion, the reported results show that, in view of a plethora of Dy-based SMMs aiming to be employed as molecular qubits, nuclear spins are indispensable ingredients to be considered in the design of SMMs. Moreover, we provide an example of nuclear-spin-based coordination chemistry exerting an effect on the global magnetic properties.

## Acknowledgements

We acknowledge the DFG-TR 88 “3Met”, and the ANR-13-BS10-0001-03 MolQuSpin. W.W. thanks the Alexander von Humboldt Foundation. We acknowledge the Karlsruhe Nano Micro Facility (KNMF, www.kit.edu/knmf) for providing access to instruments at their laboratories.

## Conflict of interest

The authors declare no conflict of interest.

**Keywords:** nuclear isotopes · quantum computing · quantum tunneling · qudits · single-molecule magnets

**How to cite:** *Angew. Chem. Int. Ed.* **2017**, *56*, 9915–9919  
*Angew. Chem.* **2017**, *129*, 10047–10051

- [1] a) R. Giraud, W. Wernsdorfer, A. M. Tkachuk, D. Maily, B. Barbara, *Phys. Rev. Lett.* **2001**, *87*, 057203; b) N. Ishikawa, M. Sugita, T. Ishikawa, S.-Y. Koshihara, Y. Kaizu, *J. Am. Chem. Soc.* **2003**, *125*, 8694–8695.
- [2] D. Gatteschi, R. Sessoli, J. Villain, *Molecular nanomagnets*, Oxford University Press, Oxford, UK, **2006**.
- [3] a) S. Thiele, F. Balestro, R. Ballou, S. Klyatskaya, M. Ruben, W. Wernsdorfer, *Science* **2014**, *344*, 1135–1138; b) S. Thiele, R. Vincent, M. Holzmann, S. Klyatskaya, M. Ruben, F. Balestro, W. Wernsdorfer, *Phys. Rev. Lett.* **2013**, *111*, 037203; c) R. Vincent, S. Klyatskaya, M. Ruben, W. Wernsdorfer, F. Balestro, *Nature* **2012**, *488*, 357–360.
- [4] D. P. O’Leary, G. K. Brennen, S. S. Bullock, *Phys. Rev. A* **2006**, *74*, 032334.
- [5] M. N. Leuenberger, D. Loss, *Nature* **2001**, *410*, 789–793.
- [6] a) K. S. Pedersen, A.-M. Ariciu, S. McAdams, H. Weihe, J. Bendix, F. Tuna, S. Piligkos, *J. Am. Chem. Soc.* **2016**, *138*, 5801–5804; b) D. Aguilà, L. A. Barrios, V. Velasco, O. Roubeau, A. Repollés, P. J. Alonso, J. Sesé, S. J. Teat, F. Luis, G. Aromorí, *J. Am. Chem. Soc.* **2014**, *136*, 14215–14222.
- [7] D. Loss, D. P. DiVincenzo, *Phys. Rev. A* **1998**, *57*, 120–126.
- [8] N. Ishikawa, M. Sugita, W. Wernsdorfer, *Angew. Chem. Int. Ed.* **2005**, *44*, 2931–2935; *Angew. Chem.* **2005**, *117*, 2991–2995.
- [9] a) J. J. Pla, K. Y. Tan, J. P. Dehollain, W. H. Lim, J. J. L. Morton, F. A. Zwanenburg, D. N. Jamieson, A. S. Dzurak, A. Morello, *Nature* **2013**, *496*, 334–338; b) F. Jelezko, T. Gaebel, I. Popa, M. Domhan, A. Gruber, J. Wrachtrup, *Phys. Rev. Lett.* **2004**, *93*, 130501.
- [10] a) L. K. Grover, *Phys. Rev. Lett.* **1997**, *79*, 325–328.
- [11] I. L. Chuang, N. Gershenfeld, M. Kubinec, *Phys. Rev. Lett.* **1998**, *80*, 3408–3411.
- [12] See: D. N. Woodruff, R. E. P. Winpenny, R. A. Layfield, *Chem. Rev.* **2013**, *113*, 5110–5148, and references therein.
- [13] See for example: a) J. Liu, Y.-C. Chen, J.-L. Liu, V. Vieru, L. Ungur, J.-H. Jia, L. F. Chibotaru, Y. Lan, W. Wernsdorfer, S. Gao, X.-M. Chen, M.-L. Tong, *J. Am. Chem. Soc.* **2016**, *138*, 5441–5450; b) R. J. Blagg, L. Ungur, F. Tuna, J. Speak, P. Comar, D. Collison, W. Wernsdorfer, E. J. L. McInnes, L. F. Chibotaru, R. E. P. Winpenny, *Nat. Chem.* **2013**, *5*, 673–678; c) J. D. Rinehart, M. Fang, W. J. Evans, J. R. Long, *Nat. Chem.* **2011**, *3*, 538–542.
- [14] a) Y. Kishi, F. Pointillart, B. Lefeuvre, F. Riobé, B. Le Guennic, S. Golhen, O. Cador, O. Maury, H. Fujiwara, L. Ouahab, *Chem. Commun.* **2017**, *53*, 3575–3578; b) F. Pointillart, K. Bernot, S. Golhen, B. Le Guennic, T. Guizouarn, L. Ouahab, O. Cador, *Angew. Chem. Int. Ed.* **2015**, *54*, 1504–1507; *Angew. Chem.* **2015**, *127*, 1524–1527.
- [15] J. M. Zadrozny, J. Niklas, O. G. Poluektov, D. E. Freedman, *J. Am. Chem. Soc.* **2014**, *136*, 15841–15844.
- [16] S. Alvarez, P. Alemany, D. Casanova, J. Cirera, M. D. Lluell, Avnir, *Coord. Chem. Rev.* **2005**, *249*, 1693.
- [17] W. Wernsdorfer, T. Ohm, C. Sangregorio, R. Sessoli, D. Maily, C. Paulsen, *Phys. Rev. Lett.* **1999**, *82*, 3903.
- [18] a) R. Marx, F. Moro, M. Dörfel, L. Ungur, M. Waters, S. D. Jiang, M. Orlita, J. Taylor, W. Frey, L. F. Chibotaru, J. V. Slagereen, *Chem. Sci.* **2014**, *5*, 3287–3293; b) N. Ishikawa, M. Sugita, T.

- Okubo, N. Tanaka, T. Iino, Y. Kaizu, *Inorg. Chem.* **2003**, *42*, 2440–2446.
- [19] a) W. Wernsdorfer, N. E. Chakov, G. Christou, *Phys. Rev. B* **2004**, *70*, 132413; b) W. Wernsdorfer, *Supercond. Sci. Technol.* **2009**, *22*, 064013.
- [20] A. Abragam, B. Bleaney, *Electron Paramagnetic Resonance of Transition Ions*, Dover, New York, **1986**, chap. 18.
- [21] W. Wernsdorfer, S. Bhaduri, R. Tiron, D. N. Hendrickson, G. Christou, *Phys. Rev. Lett.* **2002**, *89*, 197201.

Manuscript received: June 17, 2017

Accepted manuscript online: July 3, 2017

Version of record online: July 17, 2017